Influence of low temperature preanneals on dopant and defect behavior for low energy Ge preamorphized silicon

R. A. Camillo-Castillo,[a] M. E. Law, and K. S. Jones
SWAMP Center, University of Florida, Gainesville, Florida 32611

L. M. Rubin
Axcelis Technologies, Beverly, Massachusetts 01915

(Received 1 June 2003; accepted 29 September 2003; published 3 February 2004)

The hold temperature of an anneal plays a crucial role in controlling the final activation and diffusion of dopants. A study on the influence of a variety of low temperature preanneals on the behavior of dopants and defects for low energy germanium preamorphization is conducted. Si wafers are preamorphized with 1×10^{15} cm^{-2} Ge^+ at energies of 10, 12, 15, 20, and 30 keV and implanted with 1×10^{15} cm^{-2}, 1 keV B^+. Furnace preanneals are performed at 450, 550, 650, and 750 °C; the samples are subsequently subjected to a spike RTA at 950 °C. Defect analyses indicate an energy threshold above which the preanneal has an effect on the defect density. Further experiments are conducted on the 10 keV Ge^+ preamorphizing implant in which the second anneal step is conducted at 750 °C for various times. An analysis of the defect evolution with time reveals that the evolution does not follow previously reported Ostwald ripening-type behavior. The microstructure is populated with very small dot-like defects, which simply dissolve with time, suggesting that the boron may play some role in the defect evolution. © *2004 American Vacuum Society*. [DOI: 10.1116/1.1627791]

I. INTRODUCTION

The semiconductor industry is characterized by its unremitting drive to achieve smaller and faster devices. A prerequisite for progress in this realm is the production of ultrashallow, low resistance junctions. Ion implantation is capable of achieving these required shallow doped layers and has become the dominant technique for introducing dopant atoms into the silicon lattice. This nonequilibrium process is accompanied by an inherent damage to the lattice and generates a very high supersaturation of interstitials. In order to repair the lattice and activate the dopant atoms an anneal is required. During this thermal process, the excess interstitials are known to couple with the substitutional dopant atoms thereby forming mobile dopant complexes[1] which result in a transient enhanced diffusion (TED) of dopant atoms such as boron. Clustering of boron atoms with the excess interstitials at concentrations far below its equilibrium solubility in silicon[2] is another consequence.

The thermal evolution of the lattice defects has been extensively studied and it is widely accepted that submicroscopic interstitial clusters (SMICs) are precursors for the nucleation of {311}-type defects. Dislocation loops are known to evolve from the dissolution or unfaulting of these {311}.[3–6] For amorphizing implants, dislocation loop formation has been attributed to the primary defects that reside in the silicon structure near the amorphous/crystalline interface known as the end of range (EOR) defects.[7] EOR defects act both as a source and a sink for excess Si interstitials and can therefore be a driving force for TED.

Surface preamorphization is widely used prior to dopant implantation to achieve ultrashallow junctions. Germanium has gained vast acceptance as an amorphization species because of its ability to induce greater disorder in the crystal structure at lower doses than Si, owing largely to its bigger atomic size. This reduces the concentration of interstitials in the structure, which contribute to defect formation and anomalous diffusion of the boron. As the semiconductor industry continues its aggressive scaledown in accordance with the International Technology Roadmap for Semiconductors (ITRS),[8] low energy germanium implants will play a crucial role in ultrashallow junction formation and therefore an understanding of its damage evolution is essential. The goal of this study is to determine the effect of a two step anneal on the EOR defects for germanium preamorphizing implants. This two-step anneal mimics many of the hold and spike anneals proposed in the ITRS.

II. EXPERIMENT

200 mm ⟨100⟩ *n*-type Czochralski grown Si wafers are preamorphized with Ge^+ at energies 10, 12, 15, 20, and 30 keV, respectively, at a constant dose of 1×10^{15} cm^{-3}, forming a continuous amorphous layer extending from the surface. Subsequently, the amorphized wafers are implanted with 1 keV B^+ at a dose of 1×10^{15} cm^{-3}. The tilt/twist angles for each implant are 5°/0°. Post-implantation anneals comprising two stages are performed. Initial preanneals are conducted for 5 min at 450, 500, 550, 600, 650, and 750 °C in a quartz tube furnace, under dry N_2 ambient. The second anneal step consists of spike rapid thermal anneal (RTA) and is conducted in an AG Associate 210T rapid thermal annealer at 950 °C, also under dry N_2 ambient. Additional experiments are conducted for the 10 keV germanium preamor-

[a]Electronic mail: rcami@tec.ufl.edu

phizing implant for the same preanneal temperatures, however the second anneal step is conducted at 750 °C for 5, 10, and 30 min and 3 h. Plan-view transmission electron microscopy (PTEM) is utilized to analyze the defect structure and images are taken at g_{220} weak beam dark field[9,10] diffraction conditions. The quantification technique of Bharatan *et al.*[11] is employed in the defect density analysis. Cross-sectional TEM (XTEM) images, taken at g_{011} bright field diffraction condition are used to confirm amorphous layer depths as measured by variable angle spectroscopic ellipsometry (VASE) at a fixed angle of 75°. Secondary ion mass spectrometry (SIMS) is used to obtain the concentration depth profiles of B in Si via an Adept 1010 Dynamic SIMS System by Physical Electronics. The physical acquisition parameters of which are 2 kV oxygen beam at 41° with respect to the normal to the surface, a beam current of 50 nA with a raster of 250 by 250 mkm and 10% gating.

III. RESULTS AND DISCUSSION

Investigations are conducted on a series of low energy Ge^+ preamorphizing implants in Si, to determine whether a two-step anneal has an effect on the EOR defects. The amorphous layers created are in the range 250–492 Å for the 10 and 30 keV Ge^+ amorphizing energies, respectively, such that a 1 keV B^+ implant is confined to the amorphous regions. The 5 min preanneal at temperatures of 650 and 750 °C achieves total regrowth of the amorphous regions. However, the 450 and 550 °C preanneals do not fully regrow the amorphous layer. Complete regrowth is attained on application of the second anneal step.

Analysis of the defect structure for the range of energies investigated reveal that dislocation loops are the predominant defect for those samples subjected to a 950 °C spike RTA; no {311} defects are observed. This is in accordance with the kinetics of Gutierrez,[12] who utilized similar energies and doses in his investigations on germanium amorphizing implants. He determined the time constant for {311} defect dissolution at a temperature of 750 °C was 40 min for a 30 keV, 1×10^{15} cm^{-2} Ge^+ implant. Both small and elongated dislocation loops are observed to populate the structure at 20 and 30 keV energies. However, as the Ge^+ energy is lowered to 15 keV there is a drastic difference in the microstructure. The evident defects are much smaller in size and the density dwindles. In particular, at 10 and 12 keV only a few very small defects are observed, suggesting that the energy plays a role in the quantity and type of defects formed.

Defect density as a function of preanneal temperature for 15, 20, and 30 keV Ge^+ amorphizing energies are depicted in Fig. 1. The defect densities at 10 and 12 keV are too low to be quantified and therefore are not included in the diagram. Clearly there is an effect of the preanneal temperature as evidenced by the peak in the densities for both the 20 and 30 keV energies. It is also apparent that the Ge^+ preamorphizing energy has some effect on the final microstructure.

Cowern *et al.*[13] demonstrated that the interstitial supersaturation decreases with time and temperature, via inverse modeling of SMIC supersaturation derived from boron TED.

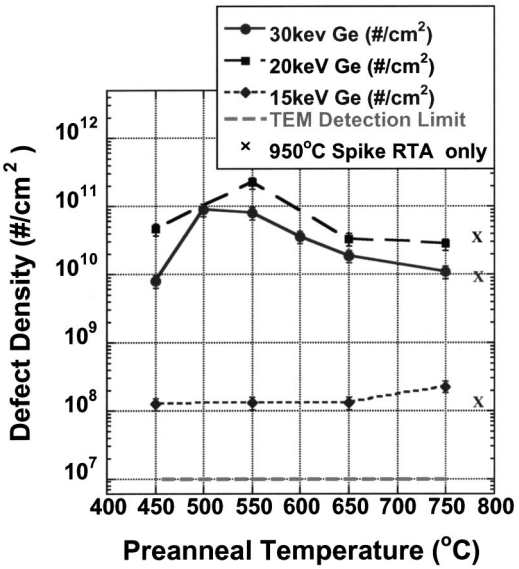

FIG. 1. Defect density vs preanneal temperature for 15, 20, and 30 keV 1×10^{15} cm^{-2} Ge^+ preamorphized Si samples containing a 1 keV, 1×10^{15} cm^{-2} B^+ implant. The samples are preannealed for 5 min at the indicated temperatures and subsequently subjected to a 950 °C spike RTA.

If the formation of SMICs is viewed as the homogenous nucleation of precipitates then the number and size of the defects is controlled by the supersaturation of the excess interstitials, consistent with Volmer and Weber's theory.[14] Hence, in the lower temperature regime there is a higher supersaturation of interstitials in the structure and therefore a larger nucleating flux. The defect density should then be smaller at the higher temperatures. For preamorphization energies exceeding 15 keV, the defect densities are seen to decrease as temperature is increased above 550 °C but the opposite trend is observed in the 450–550 °C temperature regime, where the density increases. Further examination of the microstructure reveals that the defect size increases with temperature, above 550 °C. But the opposite effect is observed when the preanneal is increased from 450 to 550 °C as smaller defects are seen at 550 °C. A similar trend is observed at 20 keV Ge preamorphization. Figure 2 shows the defects observed for 30 keV Ge preamorphization.

PTEM micrographs of the defects at 550 °C indicate a high density of small loops. Similarly at 500 °C the small loop density is high; however at 450 °C the density of small loops is much less. The lower defect density at 450 °C can be attributed to the nucleation rate of the interstitial clusters, which is temperature dependent. The nucleation at 450 °C occurs at a slower rate than at the higher temperatures and therefore there may have been insufficient time for nucleation, which would account for the lower defect density. The possibility also exists that there is sufficient time for nucleation, but the time spent in the growth regime is inadequate for the formation of clusters large enough to be resolved via PTEM. The peak that is observed in the defect density may be the result of the occurrence of two opposing effects of nucleation and dissolution.

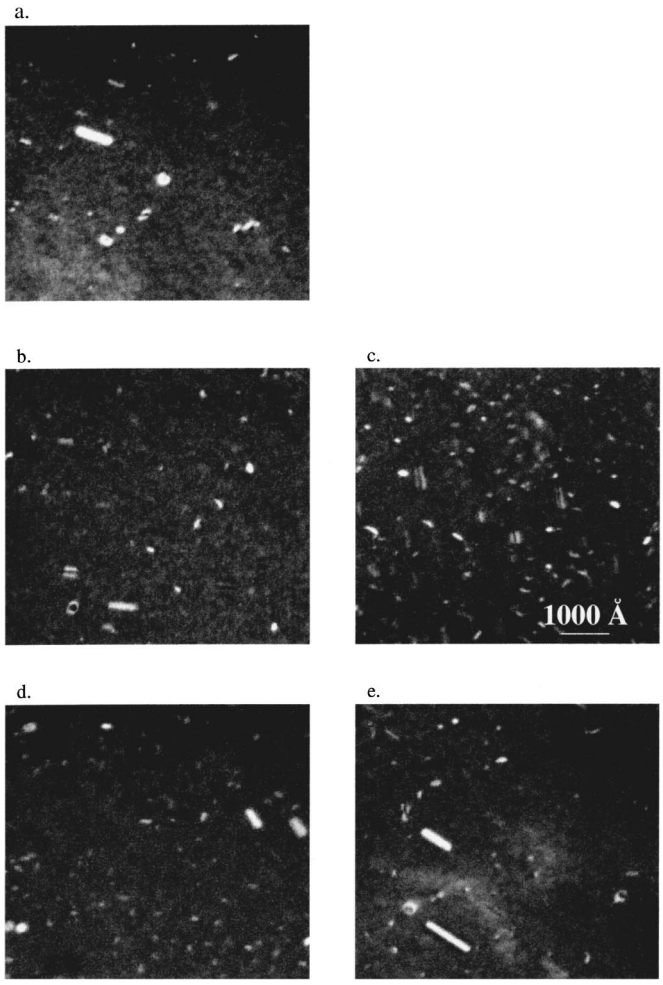

FIG. 2. PTEM WBDF images of the EOR defects observed for 1×10^{15} cm^{-2}, 30 keV Ge^+ preamorphized Si containing 1×10^{15} cm^{-2}, 1 keV B^+ and subjected to (a) 950 °C spike RTA and preanneals of (b) 450 °C, (c) 550 °C, (d) 650 °C, and (e) 750 °C followed by a spike RTA at 950 °C.

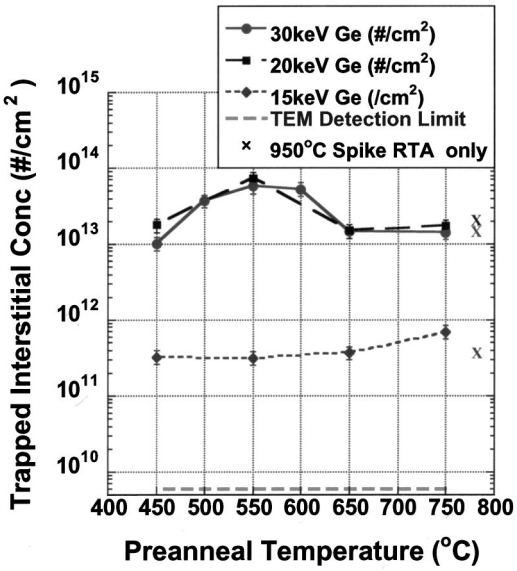

FIG. 3. Trapped interstitial concentration vs preanneal temperature for 15, 20, and 30 keV 1×10^{15} cm^{-2} Ge^+ preamorphized Si samples containing a 1 keV, 1×10^{15} cm^{-2} B^+ implant. The samples are preannealed for 5 min at the indicated temperatures and subsequently subjected to a 950 °C spike RTA.

Comparison with the trapped interstitial concentration in Fig. 3 indicates that it unmistakably adheres to a trend similar to the defect density. The maximum of the trapped interstitial population for germanium energies exceeding 15 keV occurs in the temperature range 550–600 °C. In particular at 30 keV, the trapped interstitial population remains approximately constant but the defect density falls at 600 °C. This suggests that the loops are in the coarsening regime and are undergoing conservative Ostwald ripening, in which the larger loops grow at the expense of the smaller ones. Subsequently, the trapped interstitial population decreases at 650 °C where it appears to remain approximately constant for higher temperatures. This decrease in the trapped interstitial population observed at the higher temperatures may be accounted for by a decrease in the supersaturation of interstitials and hence a smaller nucleating flux.

The effect of the preanneal is visible when the defect densities and the trapped interstitial concentrations are compared to those obtained for the control, which was not subjected to a preanneal. The preanneal noticeably results in a greater defect density and trapped interstitial population for the temperature range 500–600 °C. Notably, both the number of defects and trapped interstitials are maximum at the 550 °C preanneal temperature, which hints at a possible optimum condition for trapping interstitials. Within a 20% error the preanneal did not have a significant effect for the other temperatures investigated. It is worth noting that the defects observed for a 750 °C preanneal are geometrically very similar to those obtained for the control.

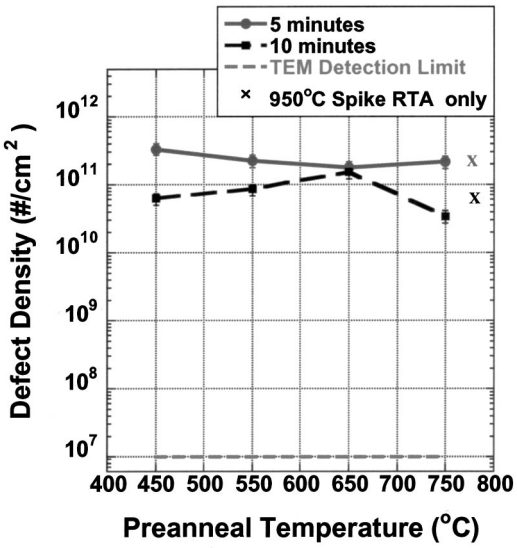

FIG. 4. Defect density vs preanneal temperature for 10 keV 1×10^{15} cm^{-2} Ge^+ preamorphized Si containing a 1 keV, 1×10^{15} cm^{-2} B^+ implant. The samples are preannealed for 5 min at the indicated temperatures and subsequently subjected a second step anneal at 750 °C for 5 and 10 min.

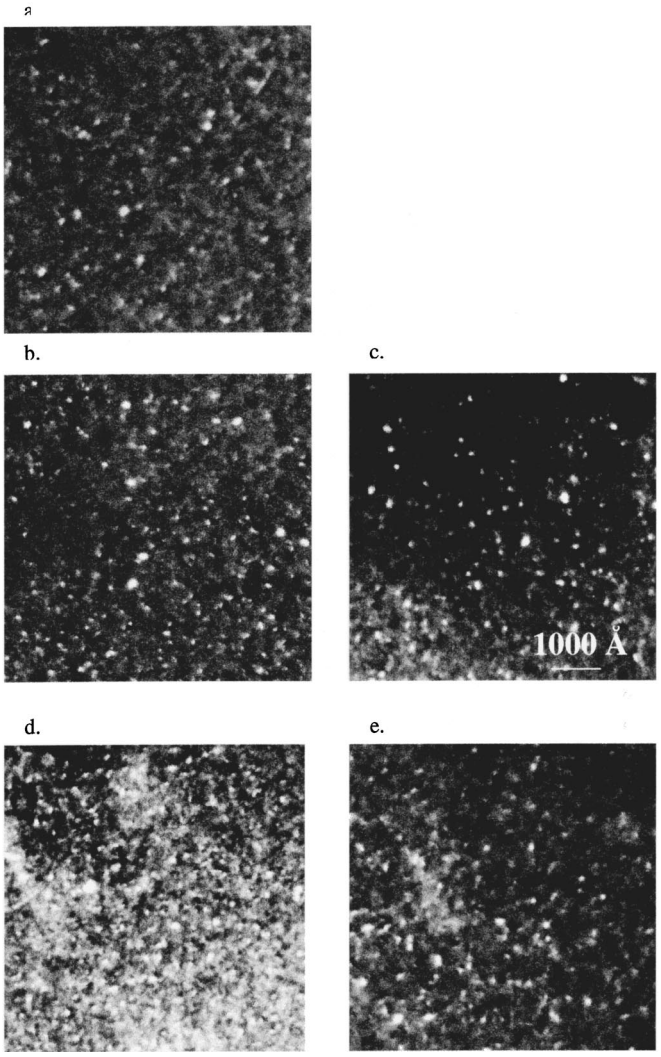

FIG. 5. PTEM WBDF images of the EOR defects observed for 1×10^{15} cm^{-2}, 10 keV Ge^+ preamorphized Si containing 1×10^{15} cm^{-2}, 1 keV B^+ subjected to the (a) 750 °C 5 min anneal and preanneals of (b) 450 °C, (c) 550 °C, (d) 650 °C, and (e) 750 °C followed by a 750 °C 5 min postanneal.

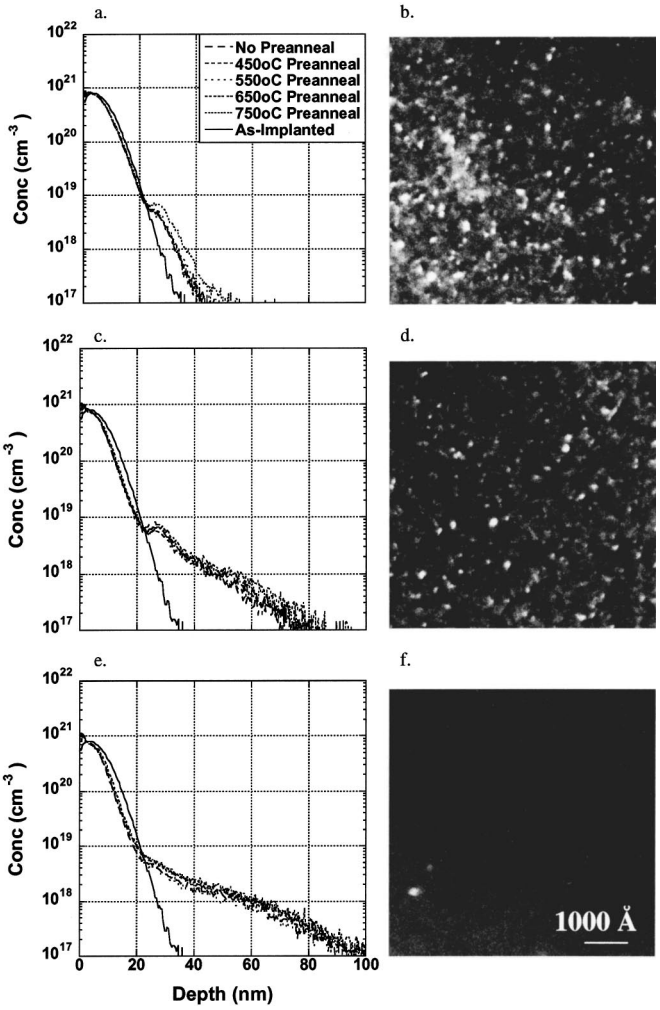

FIG. 6. SIMS concentration-depth profiles for 10 keV 1×10^{15} cm^{-2} Ge^+ preamorphized Si with a 1 keV, 1×10^{15} cm^{-2} B^+ implant subjected to no preanneal and 5 min preanneals of 450 °C, 550, 650, and 750 °C followed by a 750 °C postanneal for (a) 5 min, (c) 10 min, and (e) 30 min. PTEM WBDF images (b) 5 min, (d) 10 min, and (f) 30 min.

For amorphizing implants, the number of interstitials in the tail region of the profile includes recoils from the projected range and the "plus one" concentration (i.e., the dose). As the energy of the amorphizing implant increases, the number of recoils into the tail of the profile also increases. One can therefore expect that the number of trapped interstitials in the EOR to be greater. This is clearly not the case for the 20 and 30 keV germanium implants. The trapped populations are very similar, which may be indicative of contributions from a second source of interstitials. The drastic difference in the profiles observed at 15 keV compared to those at 20 and 30 keV germanium preamorphization energies denotes that there may be an energy threshold at which the preanneal has a significant effect on the defect dynamics. The decreased defect densities and trapped interstitial populations at 15 keV could be due largely to reduced recoils at lower energies and hence less damage in the structure. The preanneal does not appear to have any effect on the defect density at 15 keV, which remains approximately constant as the preanneal temperature is varied. The slight increase in the defect densities and trapped interstitial concentrations visible at 750 °C may not be a true artifact of the increase in temperature and should be attributed to noise.

In an attempt to explore the evolution of the defect structure for the 10 keV energy germanium preamorphization, a second step anneal temperature of 750 °C is selected based on the findings of Gutierrez.[7] His studies indicate that for a 10 keV Ge^+ amorphizing implant annealed at 750 °C, dislocation loops are the predominant defect and they are stable for ~1 h. The dislocation loops are initially very small and coalesce and grow with time, as evidenced by a steadily decreasing defect density at 5 min to anneal times up to 6 h.

PTEM analysis of those samples subject to preanneals and a second anneal at 750 °C indicate very tiny dot-like defects as being predominant throughout the structure, for the range of temperatures and times investigated. Figures 4 and 5 depictthe results of the two step anneal study of the EOR defect

density. Clearly there is no significant effect of the preanneal on the defect evolution, as the defect density remains effectively unchanged and independent of the preanneal temperature within a 20% error. It should be noted that the slight increase in the density at 650 °C for a 10 min anneal may not be a real artifact since the defects are extremely small and difficult to discern. It is evident that the defect density decreases with anneal time; being larger for the 5 min postanneal and subsequently decreasing as the anneal time is increased to 10 min. As the anneal time is extended to 30 min the defects observed are of similar size and the density is extremely low. After 3 h of annealing virtually no defects are observed.

Figure 6 shows the boron concentration-depth profiles. It is apparent that as the anneal progresses there is a pileup of boron at the EOR, indicated by the distinctive bump in the profile after a 10 min anneal at 750 °C. However, after 30 min of annealing, total dissolution of the bump is observed which suggests the EOR defects have essentially dissolved releasing the trapped boron. This correlates very well with the PTEM analysis and further emphasizes the ephemeral nature of the EOR defects.

The defect structure and evolution detected significantly differ from that reported by Gutierrez for a 10 keV Ge^+ preamorphizing implant of the same energy and dose. There is no evidence of an Ostwald ripening behavior when increasing the anneal time, rather the formation of tiny dot-like defects scattered throughout the structure, which simply dissolve with time. Recent studies by Mannino *et al.*[15] on the effect of silicon interstitial supersaturation on boron interstitial cluster (BIC) formation, demonstrate that interstitial supersaturation is considerably lower for specimens which form BICs. Owing to the reduced interstitial supersaturation, highly boron doped silicon samples do not follow the Ostwald ripening behavior observed in similar samples without boron. Gutierrez's experiments differ in that there is no subsequent B^+ implant into the Ge^+ preamorphized structure. It is therefore reasonable to hypothesize that the boron presence influences the defect evolution by clustering with the interstitial atoms. This clustering depletes the interstitial supersaturation in the vicinity of the EOR and thus inhibits the formation of {311} defects and dislocation loops. The fact that the dot-like defects appear to dissolve very quickly and are not observed after 30 min of annealing at 750 °C, suggest that these defects are not very stable. Further investigations however are required to form a conclusion as to why these dot defects are the prime defect structure.

IV. CONCLUSION

The effect of low temperature preanneals on defects and dopant diffusion for low energy Ge^+ preamorphized Si is investigated. The experimental data clearly suggest that the preanneal temperature and the Ge^+ preamorphizing energy play a crucial role in the defect behavior. For 20 and 30 keV GE^+ preamorphization energies, the highest defect densities and trapped interstitials are observed for preanneal temperatures ranging 500–600 °C. At high temperatures the lower supersaturation yields a low nucleating flux and diffusion is high. The inverse holds at low temperatures. The result may therefore be the outcome of the simultaneous counter processes of the nucleation of defects and diffusion, which are altered by varying the low temperature preanneals.

As the preamorphization energy is scaled down to less than 20 keV, the phenomenon is not apparent for a 950 °C spike anneal. Additional investigations are conducted on the 10 keV Ge^+ preamorphization energy, for a reduced postanneal temperature of 750 °C. These experiments further demonstrate no effect of the preanneal at the lower energies. They also reveal a considerably different microstructure which consists of tiny dot-like defects that dissolve in approximately 30 min. This defect behavior differs from that of previous studies which utilized similar Ge energies and doses but contained no subsequent boron implant. It is postulated that the presence of the boron inhibits the formation of the larger dislocation loops, by clustering with the interstitial atoms.

[1]P. M. Fahey, P. B. Griffin, and J. D. Plummer, Rev. Mod. Phys. **61**, 289 (1989).
[2]P. A. Stolk, H.-J. Gossmann, D. J. Eaglesham, D. C. Rafferty, G. H. Gilmer, M. Jaraiz, J. M. Poate, H. S. Luftman, and T. E. Haynes, J. Appl. Phys. **81**, 4460 (1997).
[3]L. H. Zhang, K. S. Jones, P. H. Chi, and D. S. Simons, Appl. Phys. Lett. **67**, 2025 (1995).
[4]H. G. A. Huizing, C. C. G. Visser, N. E. B. Cowern, P. A. Stolk, and R. C. M. de Kruif, Appl. Phys. Lett. **69**, 1211 (1996).
[5]J. L. Benton, S. Libertino, P. Kringhoj, D. J. Eaglesham, and J. M. Poate, J. Appl. Phys. **82**, 120 (1997).
[6]S. Coffa, S. Libertino, and C. Spinella, Appl. Phys. Lett. **76**, 321 (2000).
[7]K. S. Jones, S. Prussin, and E. R. Weber, Appl. Phys. A (USA) **34**, 1 (1988).
[8]Semiconductor Industry Association, International Technology Roadmap for Semiconductors: 2000 updated edition, Austin, TX, International SEMATECH (2000).
[9]D. B. Williams and C. B. Carter, *Transmission Electron Microscopy* (Plenum, New York, 1996), Vol. 3, p. 421.
[10]M. H. Loretto, *Electron Beam Analysis of Materials* (Chapman and Hall, London, 1984).
[11]S. Bharatan, J. Desrouches, and K. S. Jones, *Materials and Processs Characterization of Ion Implantation* (Ion Beam Press, 1997), Vol. 4, p. 222.
[12]A. F. Gutierrez, Masters thesis, Materials Science and Engineering, University of Florida, 2001, p. 16.
[13]N. E. B. Cowern, G. Mannino, P. A. Stolk, F. Rooseboom, H. G. A. Huizing, J. G. M. van Berkum, F. Cristiano, A. Claverie, and M. Jariaz, Phys. Rev. Lett. **82**, 4460 (1999).
[14]M. Volmer and A. Weber, J. Phys. Chem. **119**, 227 (1926).
[15]G. Mannino, V. Privitera, S. Solmi, and N. E. B. Cowern, Nucl. Instrum. Methods Phys. Res. B **186**, 246 (2002).